cmgh
CELLULAR AND MOLECULAR GASTROENTEROLOGY AND HEPATOLOGY

ORIGINAL RESEARCH

Critical Role of PepT1 in Promoting Colitis-Associated Cancer and Therapeutic Benefits of the Anti-inflammatory PepT1-Mediated Tripeptide KPV in a Murine Model

Emilie Viennois,[1,2] Sarah A. Ingersoll,[1] Saravanan Ayyadurai,[1] Yuan Zhao,[1,3] Lixin Wang,[1,2] Mingzhen Zhang,[1] Moon K. Han,[1] Pallavi Garg,[1] Bo Xiao,[1] and Didier Merlin[1,2]

[1]*Institute for Biomedical Sciences, Center Diagnostics and Therapeutics, Georgia State University, Atlanta, Georgia;* [2]*Veterans Affairs Medical Center, Decatur, Georgia;* [3]*Department of Gastroenterology, Zhongshan Hospital, Fudan University, China*

SUMMARY

Peptide transporter 1 (PepT1) is highly expressed in colorectal tumor biopsy specimens and exacerbates tumor development in murine models of colitis-associated cancer. The small peptide Lys-Pro-Val, transported by PepT1, decreases colon tumorigenesis, suggesting that PepT1 is a potential therapeutic target for colon cancer.

BACKGROUND & AIMS: The human intestinal peptide transporter 1 (hPepT1), is expressed in the small intestine at low levels in the healthy colon and up-regulated during inflammatory bowel disease. hPepT1 plays a role in mouse colitis and human studies have shown that chronic intestinal inflammation leads to colorectal cancer (colitis-associated cancer; CAC). Hence, we assessed here the role of PepT1 in CAC.

METHODS: Mice with hPepT1 overexpression in intestinal epithelial cells (transgenic [TG]) or PepT1 (PepT1-knockout [KO]) deletion were used and CAC was induced by azoxymethane/dextran sodium sulfate.

RESULTS: TG mice had larger tumor sizes, increased tumor burdens, and increased intestinal inflammation compared with wild-type (WT) mice. Conversely, tumor number and size and intestinal inflammation were decreased significantly in PepT1-KO mice. Proliferating crypt cells were increased in TG mice and decreased in PepT1-KO mice. Analysis of human colonic biopsy specimens showed increased expression of PepT1 in patients with colorectal cancer, suggesting that PepT1 might be targeted for the treatment of CAC. The use of an anti-inflammatory tripeptide Lys-Pro-Val (KPV) transported by PepT1 was able to prevent carcinogenesis in WT mice. When administered to PepT1-KO mice, KPV did not trigger any of the inhibitory effect on tumorigenesis observed in WT mice.

CONCLUSIONS: The observations that PepT1 was highly expressed in human colorectal tumor and that its overexpression and deletion in mice increased and decreased colitis-associated tumorigenesis, respectively, suggest that PepT1 is a potential therapeutic target for the treatment of colitis-associated tumorigenesis. *(Cell Mol Gastroenterol Hepatol 2016;2:340–357; http://dx.doi.org/10.1016/j.jcmgh.2016.01.006)*

Keywords: Colitis-Associated Cancer; Intestinal Inflammation; PepT1; KPV Peptide.

The proton-dependent oligopeptide transporter family includes 4 transporter proteins belonging to the SLC15A solute carrier group.[1] Of them, peptide transporter 1 (PepT1) is a dipeptide and tripeptide transporter that is expressed primarily in the small intestine of healthy individuals. PepT1 transports dipeptides/tripeptides from the lumen into epithelial cells via an inward-directed proton gradient.[2] Under normal physiological condition, intestinal epithelial cells show apical expression of PepT1, facilitating the transport and absorption of dipeptides/tripeptides from endogenous sources in the small intestinal epithelial cells. There are some controversies regarding whether PepT1 also is expressed in colonic tissues. Multiple studies have reported little or no PepT1 expression at messenger RNA (mRNA) levels in the colons of healthy human beings and rodents.[3–10] Other reports have suggested that PepT1 mRNAs were distributed regionally in the colon, with little or no expression in proximal colon and an increased expression in the distal colon.[5,6,11] Although another study showed PepT1 protein expression using immunofluorescence in the proximal colon at steady state, the potential transport functions of colonic PepT1 were not investigated.[11]

Despite these controversies regarding PepT1 expression during steady state, the alterations to the expression profile of PepT1 within the gastrointestinal tract during chronic inflammation have been well described. In patients with

Abbreviations used in this paper: **AOM, azoxymethane; APC, adenomatous polyposis coli; CAC, colitis-associated-cancer; DSS, dextran sodium sulfate; ERK, extracellular signal-regulated kinase; IBD, inflammatory bowel disease; IL, interleukin; IκB-α, inhibitor of κB; IκK-α/β, IκB kinase; KO, knockout; KPV, Lys-Pro-Val; mRNA, messenger RNA; NF-κB, nuclear factor κ-light-chain-enhancer of activated B cells; PepT1, peptide transporter 1; TG, transgenic; TUNEL, terminal deoxynucleotidyl transferase–mediated deoxyuridine triphosphate nick-end labeling; WT, wild-type.**

Most current article

2352-345X
http://dx.doi.org/10.1016/j.jcmgh.2016.01.006

chronic diseases, such as inflammatory bowel disease (IBD) and short-bowel syndrome, PepT1 expression is up-regulated in the colon.[7,9] Colonic PepT1 is highly expressed in interleukin (IL)$10^{-/-}$ mice with colitis but not in *Lactobacillus plantarum*–treated $IL10^{-/-}$ mice, lacking any signs of colitis.[12] It also was shown that colonic PepT1 expression and function may be induced in mice under pathologic conditions of the colon from *Citrobacter rodentium* infection.[13] In addition to dipeptides/tripeptides from the diet and other endogenous sources, PepT1 also is able to transport dipeptides/tripeptides from bacterial origin, such as N-formyl-methionine-leucine-phenylalanine,[14–19] muramyl dipeptide,[20] and L-Ala-gamma-D-Glu-mDAP.[21] Previous in vitro results from our laboratory and others have shown that bacterial peptide transport by PepT1 in colonic epithelial cells could trigger downstream proinflammatory events, including increased production of inflammatory cytokines via a nuclear factor-κB (NF-κB) pathway activation, and deregulation of colonic microRNA expression.[16,20–22] These findings suggest that PepT1 could play a crucial role in cell-to-cell communication during colitis. In the context of IBD, a functional *hPepT1* single-nucleotide polymorphism (rs2297322) recently was linked to the presence of IBD in Swedish patients free of the Nucleotide-binding oligomerization domain-containing protein 2 mutations,[23] suggesting that *hPepT1* mutation may contribute to the pathology of IBD. However, additional studies are needed to explore how this mutation affects the expression and function of PepT1 during IBD.

In 2 previous studies,[17,24] we designed transgenic (TG) mice that overexpressed PepT1 under the control of the *villin* promoter (which confers specific expression in intestinal epithelial cells) and obtained PepT1-knockout (KO) mice from Deltagene (San Mateo, CA), to examine how PepT1 overexpression or deletion affected intestinal inflammation using various models of colitis. Our results showed that overexpression of PepT1 in intestinal epithelial cells increased inflammation and exacerbated colitis pathology.[24] In dextran sodium sulfate (DSS)-treated TG mice, the degree of pathology was correlated to increased proinflammatory cytokine production, increased neutrophil infiltration, and greater weight loss compared with wild-type (WT) mice.[24] Importantly, DSS-treated PepT1-KO mice developed a moderate colitis compared with WT mice.[25] Histologic examination showed that DSS-treated PepT1-KO mice showed less proinflammatory cytokine production, neutrophil infiltration, and weight loss compared with DSS-treated WT mice. In addition, knockout of PepT1 decreased the chemotaxis of immune cells recruited to the intestine during inflammation. Finally, phenotypes observed with both TG and PepT1-KO mice were linked to the presence of gut microbiota because they were attenuated by antibiotic treatment.[24,25] Together, these findings suggested that PepT1 expression in immune cells regulates the secretion of proinflammatory cytokines triggered by bacteria and/or bacterial products, thus playing an important role in the induction of colitis.

Colorectal cancer is among the most common human malignancies[26] and has been linked firmly to chronic intestinal inflammation, giving rise to the term colitis-associated cancer (CAC).[7,27] The development of CAC in patients suffering from IBD is one of the best-characterized examples of an association between intestinal inflammation and carcinogenesis.[28–33] Among patients with ulcerative colitis, the risk of colon cancer has been found to be as high as 2% at 10 years, 8% at 20 years, and 18% at 30 years after the initial diagnosis.[28] In contrast, the lifetime risk of sporadic colorectal cancer in the United States is only 5%.[34] In the present study, we hypothesized that PepT1 could be involved in CAC development because of its role in intestinal inflammation. To test this hypothesis, we used both TG and PepT1-KO mice and used a well-known murine model of CAC using the carcinogen azoxymethane (AOM), followed by 2 cycles of DSS.[35,36] PepT1 has been shown to transport many types of drugs/prodrugs,[37–39] including Lys-Pro-Val (KPV).[40] This anti-inflammatory tripeptide, which is derived from α-melanocyte–stimulating hormone, has been shown to have anti-inflammatory properties[41,42] and to effectively reduce chemically induced colitis in mice.[40,43,44] Therefore, we hypothesized that KPV may attenuate tumorigenesis in the AOM/DSS-induced murine model of colon cancer.

In this study, we reported the effect of PepT1 overexpression and deletion in AOM/DSS-induced carcinogenesis. We interestingly observed that KPV was able to decrease the tumor number and the proliferation of malignant colonic epithelial cells in a PepT1-dependent way, confirming that PepT1 can be a therapeutic target for the treatment of colonic inflammation and subsequent tumorigenesis.

Materials and Methods

Mice

Eight-week-old female TG, PepT1-KO, and the respective WT mice with matching C57BL/6 or FVB/NJ background were used in this study. Apc^{Min} mice ($Apc^{Min/+}$), which contain a germline mutation in the adenomatous polyposis coli (APC) gene and develop multiple intestinal neoplasia (Min), were purchased from the Jackson Laboratory (Bar Harbor, ME). Mice were housed in specific pathogen-free conditions and fed ad libitum. All the experiments involving mice were approved by the Institutional Animal Care and Use Committee (Georgia State University, Atlanta, GA; permit numbers A14010 and A14007).

Colitis-Associated Cancer and Intestinal Adenoma Spontaneous Models

CAC was induced as previously described with some modifications.[45] Mice were injected intraperitoneally with AOM (10 mg/kg body weight) (Sigma-Aldrich, St. Louis, MO) diluted in phosphate-buffered saline (10 mg/kg) and maintained on regular diet and water for 5 days. Mice then were subjected to 2 cycles of DSS treatment (MP Biomedicals, Solon, OH), in which each cycle consisted of 2.5% DSS for 7 days followed by a 14-day recovery period with regular water. Mice were killed by CO_2 asphyxiation. Colonic tumors were counted and measured using a dissecting microscope. Colonic tumors were counted and grouped by size as follows: less than 1, 1–2, and more than 2 mm. The total

sum of the area of tumors for each colon was given as the tumor burden index.

In experiments testing the efficacy of KPV (Biopeptide Co, Inc, San Diego, CA) the earlier-described protocol was used with slight modifications. Five days after AOM injections (10 mg/kg or 15 mg/kg to WT or PepT1-KO, respectively), WT or PepT1-KO mice were given 3% DSS with or without KPV for 7 days, followed by 14 days of normal drinking water, then 2.5% or 3% DSS in WT or PepT1-KO mice, respectively, with or without KPV for 7 days, followed by 14 days of normal drinking water. The KPV-treated group received 100 μmol/L KPV in their drinking water along with the DSS during both DSS cycles. While receiving DSS treatment the mice were weighed daily to ensure that mice did not lose more than 20% of their original body weight.

From 5 to 18 weeks of age, $APC^{Min/+}$ mice were treated with KPV diluted to 100 μmol/L in the drinking water. Mice were killed at 18 weeks of age by CO_2 asphyxiation. The entire small intestine and colon were dissected longitudinally. Intestinal tissues were examined under a dissecting microscope and counted for the presence of adenomas. Intestinal adenomas were counted and grouped by size as follows: less than 1, 1–2, and more than 2 mm.

Human Colon Tissue Microarray

Human colon tissue array slides were purchased from US Biomax, Inc. (Rockville, MD). The microarray slide consisted of 75 samples in duplicates of normal, reactive, and cancerous (different grades and stages) colon tissues. The grading system of the tumor was as follows: grade 1 or well differentiated, cells appear normal and are not growing rapidly; grade 2 or moderately differentiated, cells appear slightly different than normal; grade 3 or poorly differentiated, cells appear abnormal and tend to grow and spread more aggressively; grade 4 or undifferentiated, features are unremarkably different from that of undifferentiated cancers of other organs. The previously described antibody against hPepT1[7] was used to stain the array slides at US Biomax, Inc, and subsequent imagings were performed by US Biomax, Inc, employees, which then were sent to our laboratory for further analysis of epithelial hPepT1 staining (rabbit h-PepT1, dilution 1:3000). Images then were scored according to 2 parameters (from 0 to 2): the intensity of the staining: 0, absence of PepT1-positive cells; 1, low-intensity staining; or 2, high-intensity staining; and the areas of positive cells in the epithelium: 0, absence of PepT1-positive cell; 1, less than the half of the epithelium was PepT1 positive; or 2, half or more of the epithelium was PepT1 positive. The intensity was indexed by the surface parameter giving one final score for each slide.

H&E Staining of Colonic Tissue

Mouse colons were fixed in 10%-buffered formalin for 24 hours at room temperature and then embedded in paraffin. Tissues were sectioned at 5-μm thickness and stained with H&E using standard protocols. Images were acquired using an Olympus microscope equipped with a DP-23 digital camera (Olympus, Pittsburgh, PA).

Immunohistochemistry

Mouse colons were fixed in formalin and paraffin-embedded. For Ki67, β-catenin, and PepT1 staining, sections were deparaffinized. Sections were incubated in sodium citrate buffer (pH 6.0) and cooked in a pressure cooker for 10 minutes for antigen retrieval. Sections then were blocked with 5% goat serum in Tris-buffered saline followed by a 1-hour incubation with anti-Ki67 (1:100; Vector Laboratories, Burlingame, CA), anti–β-catenin (1:1000; Cell Signaling, Danvers, MA), or anti-mPepT1 at 37°C. After washing with Tris-buffered saline, sections were treated with appropriate biotinylated secondary antibodies for 30 minutes at 37°C, and color development was performed using the Vectastain ABC kit (Vector Laboratories). Sections then were counterstained with hematoxylin, dehydrated, and coverslipped. Images were acquired using an Olympus microscope equipped with a DP-23 digital camera. Ki67-positive cells were counted per crypt.

Terminal Deoxynucleotidyl Transferase–Mediated Deoxyuridine Triphosphate Nick-End Labeling Staining

To quantitate the number of apoptotic cells in colonic epithelial cells, paraffin sections were deparaffinized and stained for apoptotic nuclei according to the manufacturer's instructions using the In Situ Cell Death Detection Kit (Roche Diagnostics, Indianapolis, IN). Images were acquired using an Olympus microscope equipped with a Hamamatsu black and white ORCA-03G digital camera. Terminal deoxynucleotidyl transferase–mediated deoxyuridine triphosphate nick-end labeling (TUNEL)-positive cells that overlapped with 4′,6-diamidino-2-phenylindole nuclear staining were counted per crypt.

Cytokine Expression Levels

RNA extraction and real-time reverse-transcription polymerase chain reaction. Total RNA was extracted from colonic tissues using the RNeasy mini Kit (Qiagen, Valencia, CA) according to the manufacturer's instructions. Yield and quality of RNA were verified with a Synergy 2 plate reader (BioTek, Winooski, VT). Complementary DNA was generated from the earlier-described total RNA isolated using the Maxima first-strand complementary DNA synthesis kit (Thermo Scientific, Lafayette, CO). mRNA expression was quantified by quantitative real-time reverse-transcription polymerase chain reaction using Maxima SYBR green/ROX (6-carboxyl-X-rhodamine) quantitative polymerase chain reaction Master Mix (Thermo Scientific) and the following sense and antisense primers: IL6: 5'-ACAAGTCGGAGGCT TAATTACACAT-3' and 5'-TTGCCATTGCACAACTCTTTTC-3'; CXCL2: 5'-CACTCTCAAGGGCGGTCAAA-3' and 5'-TACGATC-CAGGCTTCCCGGGT-3'; IL22: 5'-GTCAACCGCACCTTTATGCT-3' and 5'-GTTGAGCACCTGCTTCATCA-3'; IL10: 5'-GGTTGCCA AGCCTTATCGGA-3' and 5'-CTTCTCACCCAGGGAATTCA-3'; tumor necrosis factor α: 5'-AGGCTGCCCCGACTACGT-3' and 5'-GACTTTCTCCTGGTATGAGATAGCAAA-3'; and 36B4: 5'-TCCAGGCTTTGGGCATCA-3' and 5'-CTTTATCAGCTGCA CATCACTCAGA-3'. Results were normalized by using the 36B4 housekeeping gene.

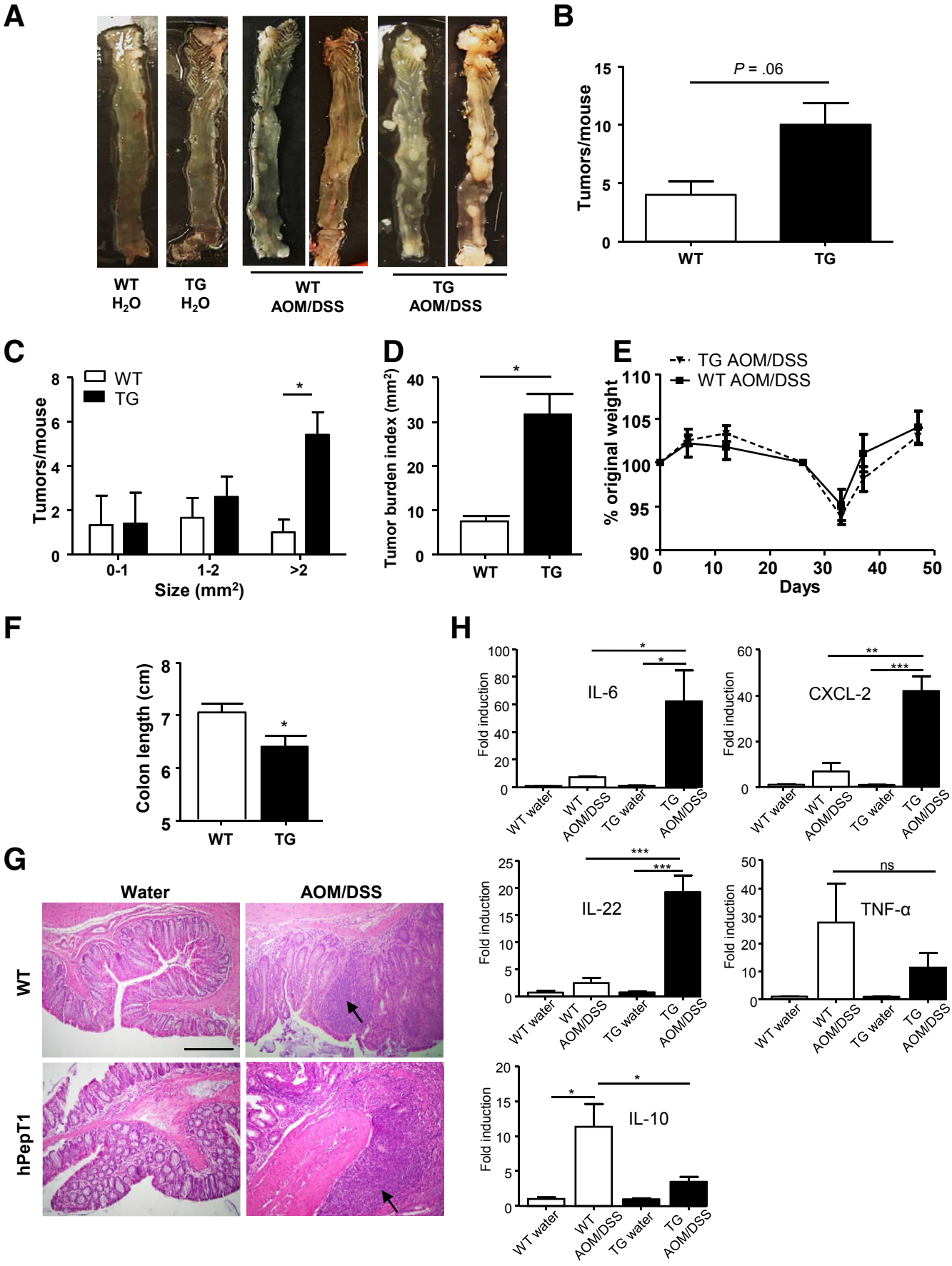
A
WT H2O
TG H2O
WT AOM/DSS
TG AOM/DSS
B
P = .06
Tumors/mouse
WT
TG
C
WT
TG
Tumors/mouse
Size (mm2)
0-1
1-2
>2
D
Tumor burden index (mm2)
E
TG AOM/DSS
WT AOM/DSS
% original weight
Days
F
Colon length (cm)
G
Water
AOM/DSS
WT
hPepT1
H
IL-6
CXCL-2
IL-22
TNF-α
IL-10
Fold induction
WT water
TG water
ns

Western Blot

Whole-colon lysates were made by homogenizing a small piece of distal colon in radioimmunoprecipitation assay buffer plus Halt phosphatase and protease inhibitor cocktail (Thermo Scientific, Inc). Fifty micrograms of lysate per well were resolved on polyacrylamide gradient gels and transferred to nitrocellulose membranes (Bio-Rad, Hercules, CA). Membranes were probed with relevant primary antibodies, including β-catenin, phosphorylated–inhibitor of κB kinase (I$\kappa\kappa$-α/β), and β-actin (Cell Signaling), mouse PepT1 (mPepT1), phosphorylated–extracellular signal-regulated kinase (ERK)1/2, and total ERK1/2 (Santa Cruz Biotechnology, Inc, Santa Cruz, CA), followed by incubation with appropriate horseradish-peroxidase–conjugated secondary antibodies (GE Healthcare Biosciences, Pittsburgh, PA). Blots were developed using enhanced chemiluminescence Western Blot detection reagents (GE Healthcare Biosciences). Densitometry quantifications were performed using the software Quantity One (Bio-Rad).

Statistical Analysis

Data are presented as means ± SEM. Statistical analysis for significance was determined using an analysis of variance test followed by a Bonferroni post-test (GraphPad Prism, La Jolla, CA).

Results

Tumor Growth Is Increased in Mice That Overexpress PepT1 in Intestinal Epithelial Cells

We first examined if PepT1 overexpression in the colon could contribute to the development of CAC because it was shown previously that TG mice had increased inflammation and exacerbated pathologies during acute colitis.[24] Our laboratory previously generated TG mice that overexpress PepT1 under the control of the *villin* promoter,[24] which is active primarily in intestinal epithelial cells. When these mice were treated with AOM/DSS, they tended to develop an increased number of tumors compared with WT mice, although this did not reach statistical significance ($P = .06$), reflecting an important variability between individuals (Figure 1*A* and *B*). The number of large tumors (>2 mm^2) was highly increased in TG vs WT mice (Figure 1*C*), as was the overall tumor burden index (ie, the total area of tumors per colon) (Figure 1*D*), which is indicative of increased susceptibility to tumorigenesis in TG mice, with an enhanced tumor growth and/or tumor cell survival. Despite the absence of any difference in body weight loss between WT and TG mice during the AOM/DSS protocol (Figure 1*E*), the colon lengths were decreased in TG mice compared with WT mice treated by AOM/DSS, showing that the TG mice were more susceptible to colitis (Figure 1*F*). Histologic examination showed the presence of larger adenomas and increased areas of inflammatory cell infiltration (arrow, Figure 1*G*) in colonic sections from AOM/DSS-treated TG and WT mice (Figure 1*G*), with increased dysplasia, aberrant crypt foci, and cellular infiltration in the colonic epithelia of AOM/DSS-treated TG mice compared with WT mice. Histologically, we did not observe any difference between water-treated (control) TG and WT mice. Next, we determined the mRNA expression levels of proinflammatory cytokines and chemokines and found the levels of *Il6*, *Cxcl2*, and *Il22* to be significantly higher in AOM/DSS-treated TG mice compared with treated WT mice (Figure 1*H*), supporting the previous observation that TG mice were more sensitive to intestinal inflammation and tumorigenesis induced by AOM/DSS treatment. Interestingly, the expression level of mRNA encoding tumor necrosis factor α, a proinflammatory cytokine reported to have an increased expression in colitis and CAC,[46] did not differ significantly between TG and WT mice (Figure 1*H*). The anti-inflammatory cytokine IL10 expression was decreased in AOM/DSS-treated TG mice compared with similarly treated WT mice (Figure 1*H*). In control (water-treated) TG and WT mice, no significant difference of these cytokine levels were observed (Figure 1*H*). Taken together, these data indicate that TG mice are more susceptible to AOM/DSS treatment than WT mice, suggesting a potential role of PepT1 in the initiation and exacerbation of cancer development.

Overexpression of hPepT1 Deregulates Proliferation and Apoptosis

The increase in tumor burden and average tumor size in TG mice suggested that they may be subjected to increased cell proliferation compared with WT mice. Proliferation of the colonic epithelial cells was analyzed using an antibody against the nuclear marker Ki67. No significant difference in the cellular proliferation between water-treated WT and TG mice was observed (Figure 2*A* and *B*). However, after AOM/DSS treatment, the number of Ki67-positive cells was

Figure 1. (***See previous page***). **Inflammation and tumor growth is increased in mice that overexpress PepT1 in their intestinal epithelial cells.** FVB/NJ WT and TG mice were injected intraperitoneally with AOM (10 mg/kg body weight), maintained for 7 days, and then subjected to a 2-cycle DSS treatment (each cycle consisted of 7 days of 2.5% DSS and 14 days of H_2O). (*A*) Representative colon samples were obtained from each experimental group at the end of the AOM/DSS protocol. (*B*) Number of tumors per mouse. (*C*) Tumor size was determined using a dissecting microscope fitted with an ocular micrometer. The tumor size distribution was graphed. (*D*) Tumor areas for each colon were summed and were presented as the tumor burden index. (*E*) AOM/DSS-treated WT and TG mice were weighed on day 0, daily during each DSS treatment, and once per week during the 2-week recovery period after each DSS treatment. The graph represents the percentage values of the original day 0 weights. (*F*) Colon lengths of AOM/DSS-treated WT and TG mice. (*G*) Representative images of H&E-stained colonic sections from WT or TG mice that received AOM/DSS or water (control). (*H*) The colonic mRNA levels of *Il6*, *Cxcl-2*, *Il22*, *Il10*, and *Tnf*-α were quantified by quantitative real-time reverse-transcription polymerase chain reaction and normalized to mRNA levels of the ribosomal protein, 36B4. Values are means ± SEM (n = 5 per group). *Scale bar*: 100 μm. *Arrow*, inflammatory cell infiltration. *$P < .05$, **$P < .01$, and ***$P < .001$.

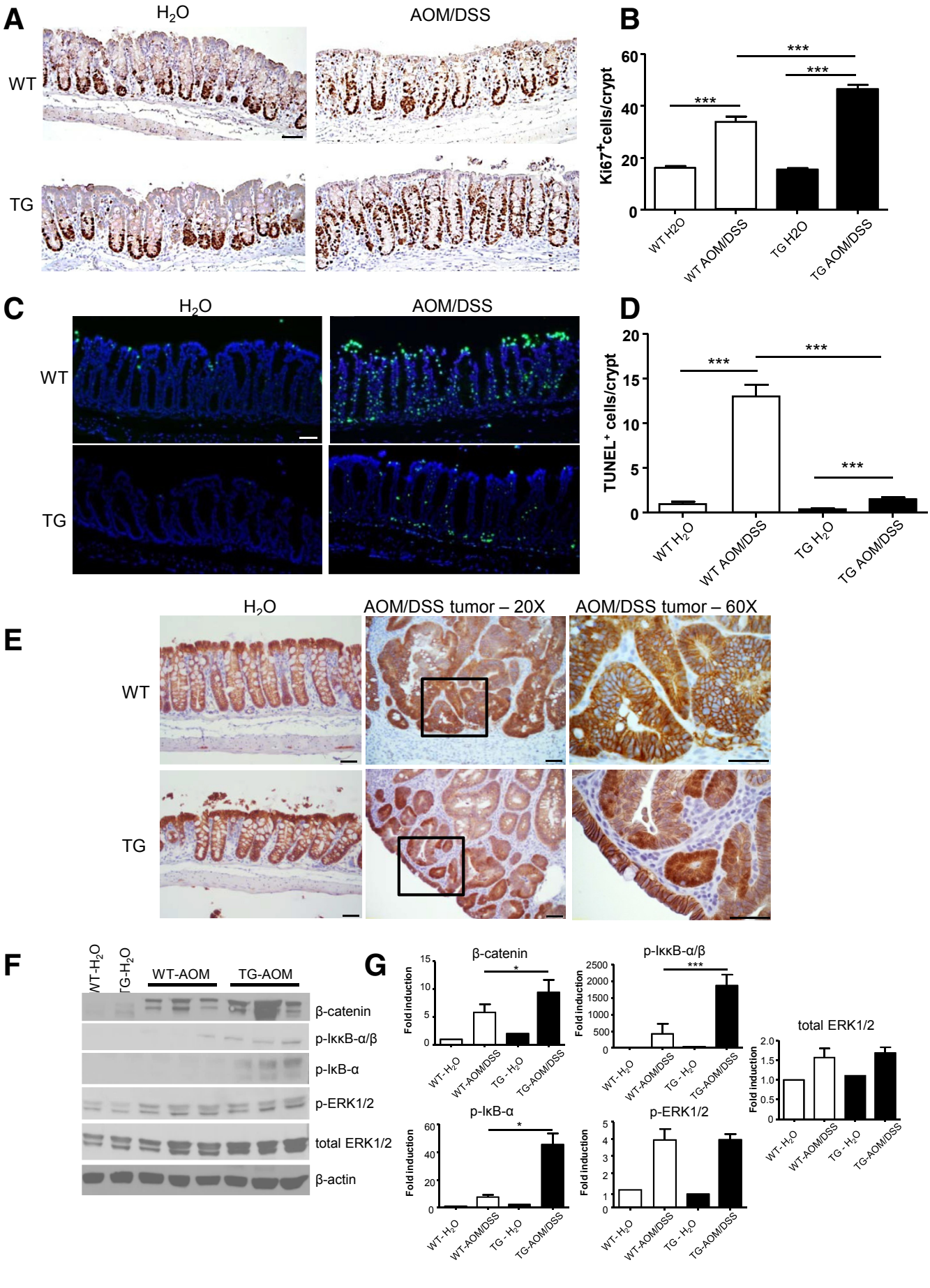
A
H2O
AOM/DSS
WT
TG
B
Ki67+cells/crypt
60
40
20
0
***
***
***
WT H2O
WT AOM/DSS
TG H2O
TG AOM/DSS
C
H2O
AOM/DSS
WT
TG
D
TUNEL+ cells/crypt
20
15
10
5
0
***
***
***
WT H2O
WT AOM/DSS
TG H2O
TG AOM/DSS
E
H2O
AOM/DSS tumor – 20X
AOM/DSS tumor – 60X
WT
TG
F
WT-H2O
TG-H2O
WT-AOM
TG-AOM
β-catenin
p-IκκB-α/β
p-IκB-α
p-ERK1/2
total ERK1/2
β-actin
G
β-catenin
p-IκκB-α/β
p-IκB-α
p-ERK1/2
total ERK1/2
Fold induction
WT-H2O
WT-AOM/DSS
TG-H2O
TG-AOM/DSS

increased in both WT and TG mice, but to a significantly higher level in TG mice compared with WT mice (Figure 2*A* and *B*). This observation indicates that overexpression of PepT1 in intestinal epithelial cells exacerbates the AOM/DSS-induced proliferation of crypt cells in the colonic epithelium. Ki67-positive cells were highly prevalent in the colon tumors of both WT and TG mice (data not shown). In addition, a TUNEL-based quantification of apoptosis in colonic sections from WT and TG mice showed that the epithelia of AOM/DSS-treated WT mice had significantly more TUNEL-positive cells compared with treated TG mice (Figure 2*C* and *D*). Although AOM/DSS treatment increased the number of apoptotic cells in both WT and TG mice, the fold change was significantly higher in the former (Figure 2*D*), indicating that PepT1 overexpression in epithelial cells minimized AOM/DSS-induced apoptosis in the colonic epithelia. Together, these data showed that PepT1 overexpression in intestinal epithelia may induce various pathways that lead to increased proliferation and/or decreased apoptosis of colonic epithelial cells, thereby potentially contributing to the increased tumor burden observed in TG mice.

Overexpression of hPepT1 Alters Tumorigenesis Signaling Pathways

Several signaling pathways have been associated with the regulation of tumorigenesis in the AOM/DSS CAC mouse model and human CAC. Among them, β-catenin is an oncogenic protein that plays important roles in cell adhesion and in a co-transcriptional activation of genes of the Wnt signaling pathway (eg, *c-myc*, *cyclooxygenase-2*, *metalloproteinase-7*, and *cyclin D1*).[47] AOM induces mutations of β-catenin at specific serine and threonine residues that are targeted by Glycogen synthase kinase-3β phosphorylation, leading to the cellular accumulation of β-catenin.[35] β-catenin immunohistochemical staining showed that the levels of free β-catenin were increased in the cytoplasm of tumor cells from AOM/DSS-treated WT and TG mice compared with control (water-treated) animals, in which the majority of β-catenin staining was associated with the cellular membranes (Figure 2*E*). We also observed an increased nuclear accumulation of β-catenin in tumor cells from TG mice compared with WT mice (Figure 2*E*), suggesting that the transcription of β-catenin may be enhanced in these cells. Consistent with these results, AOM/DSS-treated WT and TG mice had increased levels of β-catenin compared with their water-treated counterparts, and β-catenin expression was slightly higher in colon lysates from TG mice compared with WT mice, as shown in the densitometric analysis of Western blot (Figure 2*F* and *G*). The NF-κB and mitogen-activated protein kinase pathways also have been implicated in colon tumorigenesis,[35,48] so we next examined associated signaling partners of these pathways by Western blot. Levels of phosphorylated IκκB-α/β and phosphorylated inhibitor of κB (IκB-α) were highly increased in AOM/DSS-treated TG mice, but only marginally in comparably treated WT mice (Figure 2*F* and *G*), suggesting that NF-κB signaling is enhanced in AOM/DSS-treated TG mice compared with WT mice. Finally, we observed increased levels of phosphorylated ERK1/2 in AOM/DSS-treated WT and TG mice compared with their respective water controls (Figure 2*F* and *G*), but found no significant AOM/DSS treatment effect between the 2 genotypes, suggesting that this pathway was not be required for the increased tumor growth observed in PepT1 TG mice.

Tumorigenesis is Decreased in PepT1-Deficient Mice

Next, we investigated whether the absence of PepT1 could protect from AOM/DSS-induced CAC phenotype. After AOM/DSS treatment, PepT1-KO mice developed significantly fewer tumors (of all sizes) compared with similarly treated WT mice (Figure 3*A*–*C*). Consistent with these data, the overall tumor burden was significantly lower in AOM/DSS-treated PepT1-KO mice compared with AOM/DSS-treated WT mice (Figure 3*D*). These data suggest that, in the absence of PepT1, mice were protected from tumor initiation and growth. Because intestinal inflammation is known to be a central factor in the initiation and development of colon tumors, we next measured various parameters of inflammation after the induction of CAC in WT and PepT1-KO mice. Monitoring of body weight showed that WT mice underwent a dramatic weight loss during the first cycle of DSS, whereas no such effect was observed in PepT1-KO mice (Figure 3*E*). The colons were longer in PepT1-KO AOM/DSS-treated compared with the WT counterpart, confirming that the PepT1-KO mice were more resistant to colitis than WT mice (Figure 3*F*). Histologic examination showed the presence of large adenomas with major lymphocyte infiltration in colonic sections from AOM/DSS-treated WT mice (Figure 3*G*), whereas no lymphocyte infiltration or adenoma was detected in AOM/DSS-treated

Figure 2. (***See previous page***). **Overexpression of hPepT1 increases colonic epithelial proliferation, decreases epithelial apoptosis, and alters tumorigenesis signaling pathways.** (*A*) The levels of epithelial cell proliferation in colonic tissue sections from WT and TG mice treated with AOM/DSS or water alone were assessed by immunohistochemistry using the proliferation marker Ki67. (*B*) $Ki67^+$ cells were counted and averaged per crypt. Values are means ± SEM (n = 5 per group). (*C*) Apoptotic colonic epithelial cells were quantified using a TUNEL assay (fluorescein isothiocyanate, green) and nuclei were stained with 4′,6-diamidino-2-phenylindole (blue). (*D*) Cells positive for both TUNEL and 4′,6-diamidino-2-phenylindole staining were counted and averaged per crypt. Values are means ± SEM (n = 5 per group). (*E*) The levels of β-catenin were assessed by immunohistochemical analysis of colonic tissue sections from WT and TG mice treated with AOM/DSS or water alone. (*F*) The protein levels of phosphorylated IκκB-α/β, phosphorylated IκB-α, β-catenin, phosphorylated-ERK1/2, and total ERK1/2 in the colons of WT or TG mice treated with AOM/DSS or water alone were analyzed by Western blot. (*G*) *Bar graph* represents densitometric quantifications of Western blot normalized to β-actin. *Scale bars*: 50 μm. $^*P < .05$, $^{***}P < .001$.

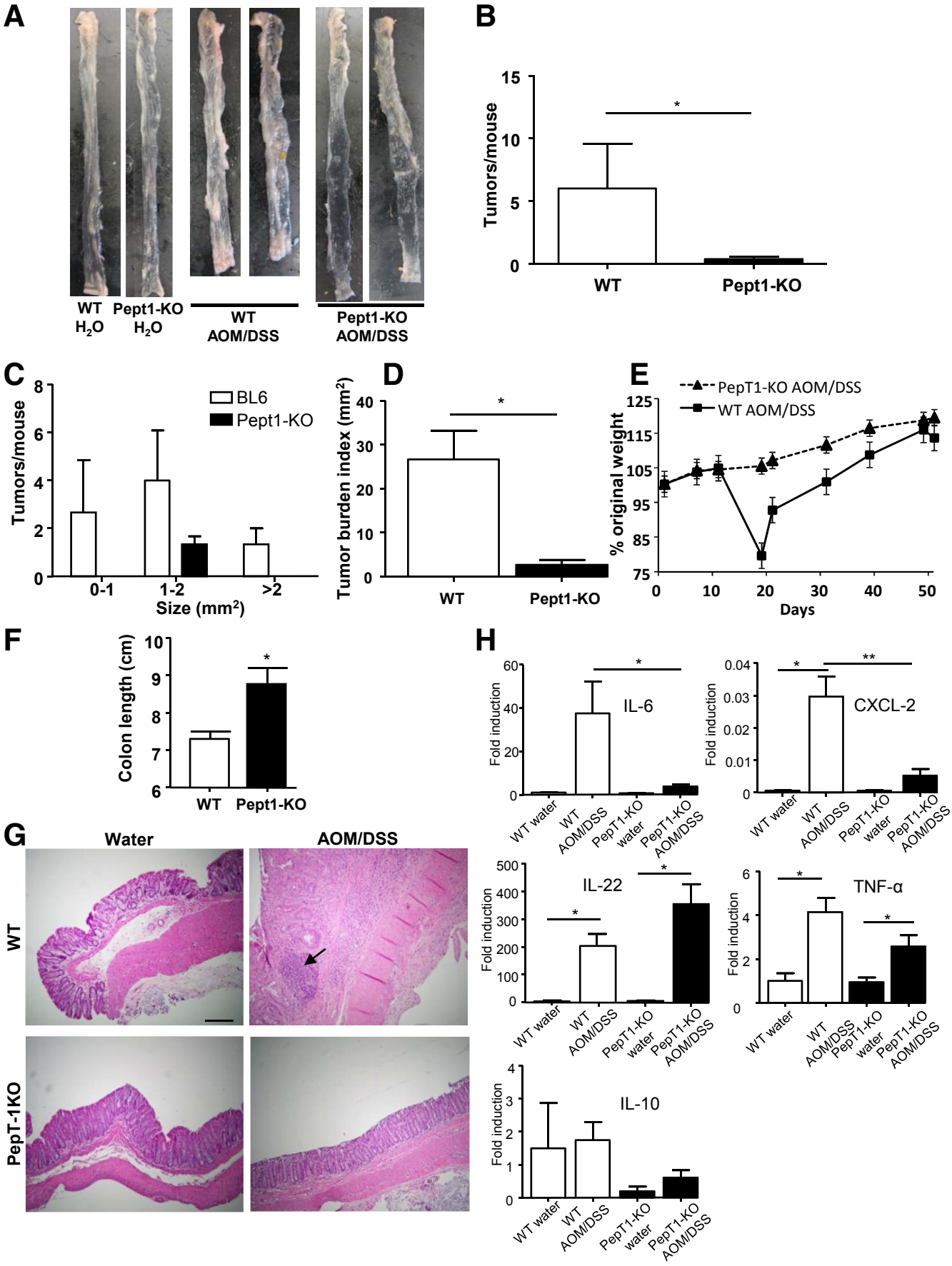
A
WT H2O
Pept1-KO H2O
WT AOM/DSS
Pept1-KO AOM/DSS
B
Tumors/mouse
WT
Pept1-KO
C
Tumors/mouse
BL6
Pept1-KO
0-1
1-2
>2
Size (mm2)
D
Tumor burden index (mm2)
WT
Pept1-KO
E
PepT1-KO AOM/DSS
WT AOM/DSS
% original weight
Days
F
Colon length (cm)
WT
Pept1-KO
G
Water
AOM/DSS
WT
PepT-1KO
H
IL-6
CXCL-2
IL-22
TNF-α
IL-10
Fold induction
WT water
WT AOM/DSS
PepT1-KO water
PepT1-KO AOM/DSS

PepT1-KO mice (Figure 3*G*). We did not observe any difference of these parameters between control (water-treated) PepT1-KO and WT mice (Figure 3*G*). Next, we examined the mRNA levels of proinflammatory cytokines and chemokines in WT and PepT1-KO mice with or without CAC induction. We found that the expression levels of *Il6*, *Cxcl2*, *Il22*, and *Tnf-α* were increased significantly in WT mice after AOM/DSS treatment. Importantly, although *Il-6* and *Cxcl-2* were increased only moderately in AOM/DSS-treated PepT1-KO mice, levels of *Il22* and *Tnf-α* were increased significantly (Figure 3*H*). The expression level of *Il10* in PepT1-KO mice tended to be lower than that in WT mice, but no significant difference was observed regardless of the genotype or treatment (Figure 3*H*). These results showed that AOM/DSS-associated intestinal inflammation was attenuated in PepT1-KO mice compared with WT mice.

Taken together, these data indicate that PepT1-KO mice were protected against AOM/DSS-induced tumorigenesis through a partial inhibition of tumorigenic intestinal inflammation. This supports our hypothesis that PepT1 plays a central role in the initiation and exacerbation of CAC in mice.

PepT1-KO Mice Elicit a Beneficial Balance of Proliferation and Apoptosis in the Colonic Mucosa Associated With Inhibition of Tumorigenesis-Related Signaling

Ki67 staining showed that there was no significant difference in cellular proliferation among water-treated (control) WT and PepT1 mice, as well as AOM/DSS-treated PepT1-KO mice, whereas AOM/DSS-treated WT mice had significantly more Ki67-positive cells per crypt (Figure 4*A* and *B*). This indicates that, in the absence of PepT1, proliferation of crypt epithelial cells was inhibited. Importantly, Ki67-positive cells were located in the entire crypt in WT mice, whereas they were located only in basal crypts in PepT1-KO mice, attesting to the extensive proliferation occurring in WT mice when subjected to AOM/DSS. Next, we used TUNEL staining to determine the levels of apoptosis in colonic mucosa sections from WT and PepT1-KO mice. The basal level of apoptosis was slightly but significantly higher in PepT1-KO mice compared with WT mice, and the number of apoptotic cells in the epithelia of WT and, to a lesser extent, PepT1-KO mice was significantly greater after AOM/DSS treatment (Figure 4*C* and *D*). Thus, PepT1 deficiency appears to be protective against the proliferative and abnormal apoptosis status induced by AOM/DSS treatment.

To investigate whether PepT1 deficiency inhibits tumorigenesis signaling pathways, the accumulation of proteins involved in tumorigenesis was analyzed by Western blot. Increased levels of phosphorylated Iκκ-α/β were observed in AOM/DSS-treated PepT1-KO mice compared with AOM/DSS-treated WT mice, whereas no difference was observed in the levels of phosphorylated IκB-α and total IκB-α between the 2 genotypes (Figure 4*E* and *F*), suggesting that the inhibition of the NF-κB pathway was not the mechanism underlying the attenuated tumor growth associated with PepT1 deficiency. Compared with the relevant controls, β-catenin levels were unaltered in AOM/DSS-treated WT mice and comparably treated PepT1-KO mice, whereas the levels of phosphorylated ERK1/2 were increased drastically in AOM/DSS-treated WT mice but remained unchanged in AOM/DSS-treated PepT1-KO mice (Figure 4*E* and *F*). This finding suggests that PepT1 deficiency may antagonize and/or protect from the AOM/DSS-induced ERK pathway. Together, these results suggest that inhibition of the tumor-growth–promoting ERK pathway[49,50] might be involved in the inhibition of AOM/DSS-associated tumor growth observed in PepT1-KO mice.

KPV Prevents Intestinal Inflammation and Tumorigenesis During Colitis-Associated Carcinogenesis in a PepT1-Dependent Manner

The analysis of PepT1 expression at the mRNA and protein levels both indicated that PepT1 levels were up-regulated in the colons of AOM/DSS-treated WT mice (Figure 5*A* and *C*). WT mice treated with AOM/DSS had increased PepT1 staining in epithelial cells lining the colon compared with water-treated (control) mice (Figure 5*B*). These immunohistochemical data were verified further by Western blot analysis of whole-colon lysates (Figure 5*C*), in which greater PepT1 expression was found in the colon of AOM/DSS-treated WT animals. Therefore, we predicted that colonic PepT1 also would be up-regulated in colon cancer patients, as previously described for bladder cancer specimens at mRNA levels.[51] To determine if PepT1 was up-regulated during human disease, we analyzed a human tissue microarray, stained for hPepT1, that included

Figure 3. (***See previous page***). **Inflammation and tumor growth is reduced in PepT1-KO mice.** WT and PepT1-KO mice were injected intraperitoneally with AOM (10 mg/kg body weight) and maintained for 7 days, then subjected to 2-cycle DSS treatment, with each cycle consisting of 7 days of 2.5% DSS and 14 days of H_2O. (*A*) Representative colons were obtained from each experimental group at the end of the AOM/DSS protocol. (*B*) Number of tumors per mouse. (*C*) Tumor size was determined using a dissecting microscope fitted with an ocular micrometer. The tumor size distribution was graphed. (*D*) Tumor areas were summed for each colon, and were presented as the tumor burden index. (*E*) AOM/DSS-treated WT and PepT1-KO mice were weighed on day 0, daily during each DSS treatment, and once per week during each 2-week post-DSS recovery period. The *graph* represents the percentage values of the original day 0 weights. (*F*) Colon lengths of AOM/DSS-treated WT and PepT1-KO mice. (*G*) Representative images of H&E-stained colonic sections from WT or PepT1-KO mice treated with AOM/DSS or water alone. (*H*) The colonic mRNA levels of IL6, CXCL-2, IL22, IL10, and tumor necrosis factor (TNF)-α were quantified by quantitative real-time reverse-transcription polymerase chain reaction and normalized to mRNA levels of the ribosomal protein, 36B4. Values are means ± SEM (n = 4–11 per group). *Scale bar*: 50 μm. *Arrow*: inflammatory cell infiltration. $^{*}P < .05$, $^{**}P < .01$.

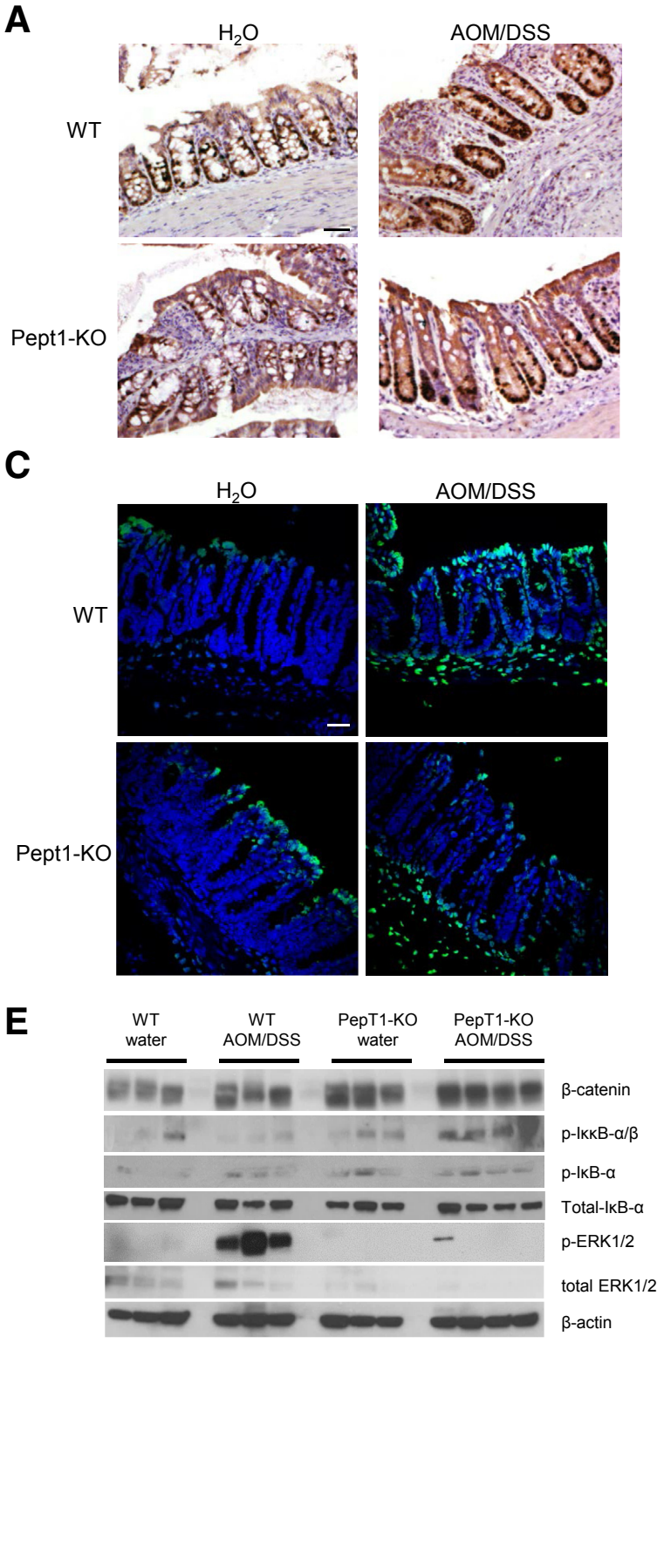
A
H2O
AOM/DSS
WT
Pept1-KO
B
Ki67+/ crypt
40
30
20
10
0
*
WT H2O
WT AOM/DSS
Pept1-KO H2O
Pept1-KO AOM/DSS
C
H2O
AOM/DSS
WT
Pept1-KO
D
TUNEL+ cells/crypt
10
8
6
4
2
0
**
***
***
*
WT H2O
WT AOM/DSS
Pept1-KO H2O
Pept1-KO AOM/DSS
E
WT water
WT AOM/DSS
PepT1-KO water
PepT1-KO AOM/DSS
β-catenin
p-IκκB-α/β
p-IκB-α
Total-IκB-α
p-ERK1/2
total ERK1/2
β-actin
F
β-catenin
p-IκκB-α/β
p-IκB-α
IκB-α
p-ERK1/2
total ERK1/2
Fold induction
WT-H2O
WT – AOM/DSS
PepT1-KO - H2O
PepT1-KO – AOM/DSS

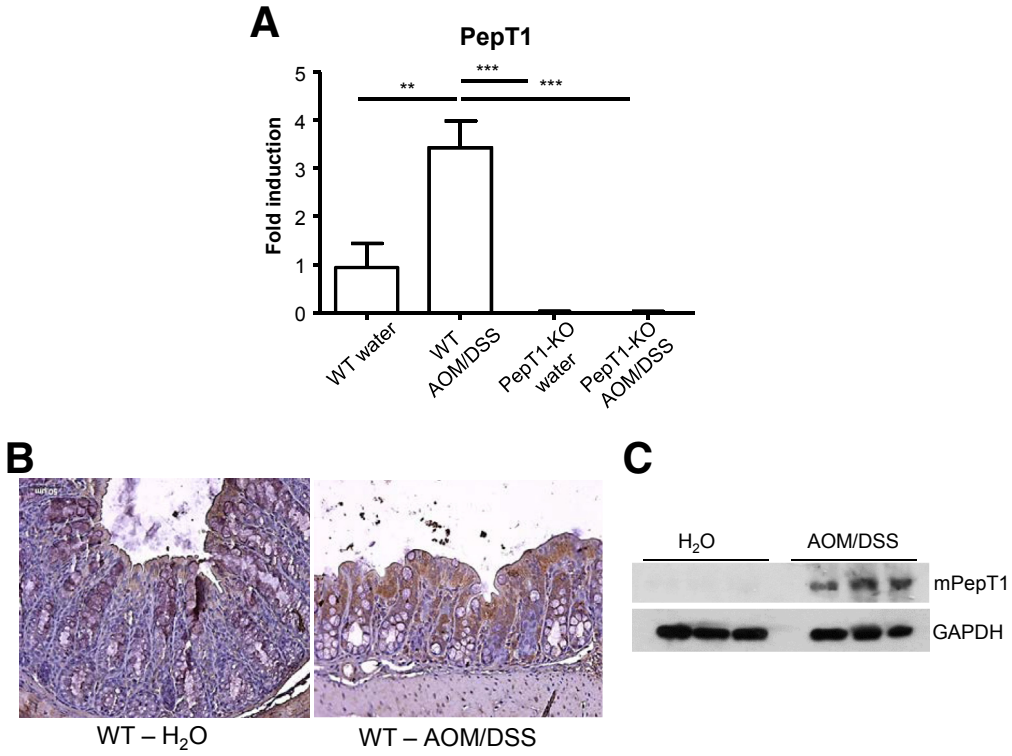

Figure 5. PepT1 expression is up-regulated during colon cancer in mice. (*A*) The colonic mRNA levels of PepT1 were quantified by quantitative real-time reverse-transcription polymerase chain reaction and normalized to mRNA levels of the ribosomal protein 36B4. Values are means ± SEM (n = 8–9 per group). (*B*) Immunohistochemical analysis of mouse PepT1 was performed on colonic tissue sections from WT mice treated with AOM (10 mg/kg body weight) plus 2 cycles of 2.5% DSS, or water alone. Microscopic images were taken at 20× magnification. (*C*) Whole-colon lysates were used in Western blot analyses for mouse PepT1. β-actin was detected as the loading control. $^{**}P < .01$, $^{***}P < .001$. GAPDH, glyceraldehyde-3-phosphate dehydrogenase.

paraffin-embedded samples from control patients and colon cancer patients with various stages of malignancies from grades I to III, as well as patients with benign colon tumors (male and female patients ranging in age from 19 to 92 years). The images then were analyzed and scored for epithelial/tumor cell hPepT1 staining. Most of the colon cancer patients showed hPepT1 staining in their epithelial and/or tumor cells (Figure 6). In normal colon samples, some hPepT1 staining was observed in cells surrounding the epithelium, which most likely were immune cells.[15] In the benign colon adenoma, hPepT1 staining was observed in limited areas of epithelia, probably as a consequence of inflammation, as previously reported.[7] Importantly, the majority of the colon tumor samples showed increased staining relative to both normal and benign tissues (Figure 6*B*). The specific up-regulation of PepT1 in tumor tissues showed the potential use of PepT1 transporter activity in the treatment of CAC.

Several studies have shown previously that KPV tripeptide decreased intestinal inflammation and attenuated DSS-induced colitis,[40,43,44] suggesting tripeptide as a valuable therapeutic tool against colitis and associated carcinogenesis. We previously showed that KPV was transported via PepT1 in vitro in Caco-2/brush border expressing (BBE) cells.[40] We then hypothesized that KPV may help to prevent colon tumorigenesis in the AOM/DSS-induced CAC model. To test this hypothesis, WT mice were treated with AOM/DSS or AOM/DSS + KPV, showing that WT mice given KPV in conjunction with AOM/DSS showed a drastic decrease in

Figure 4. (*See previous page*). PepT1 knockout decreases colonic epithelial proliferation, modifies epithelial apoptosis, and inhibits tumorigenesis-related signaling. (*A*) The levels of epithelial cell proliferation in colonic tissue sections from WT and PepT1-KO mice treated with AOM/DSS or water alone were assessed by immunohistochemistry using the proliferation marker Ki67. (*B*) $Ki67^{+}$ cells were counted and averaged per crypt. Values are means ± SEM (n = 5–9 per group). (*C*) Apoptotic colonic epithelial cells were quantified using a TUNEL assay (fluorescein isothiocyanate, green), and nuclei were stained with 4′,6-diamidino-2-phenylindole (blue). (*D*) Cells positive for both TUNEL and 4′,6-diamidino-2-phenylindole were counted and averaged per crypt. Values are means ± SEM (n = 5–9 per group). (*E*) The protein levels of phosphorylated IκκB-αβ, phosphorylated and total IκB-α, β-catenin, phosphorylated-ERK1/2, and total ERK1/2 in the colons of WT or PepT1-KO mice treated with AOM/DSS or water alone were analyzed by Western blot. (*F*) *Bar graph* represents densitometry quantifications of Western blot normalized to β-actin. *Scale bars*: 50 μm. $^{*}P < .05$, $^{**}P < .01$, and $^{***}P < .001$.

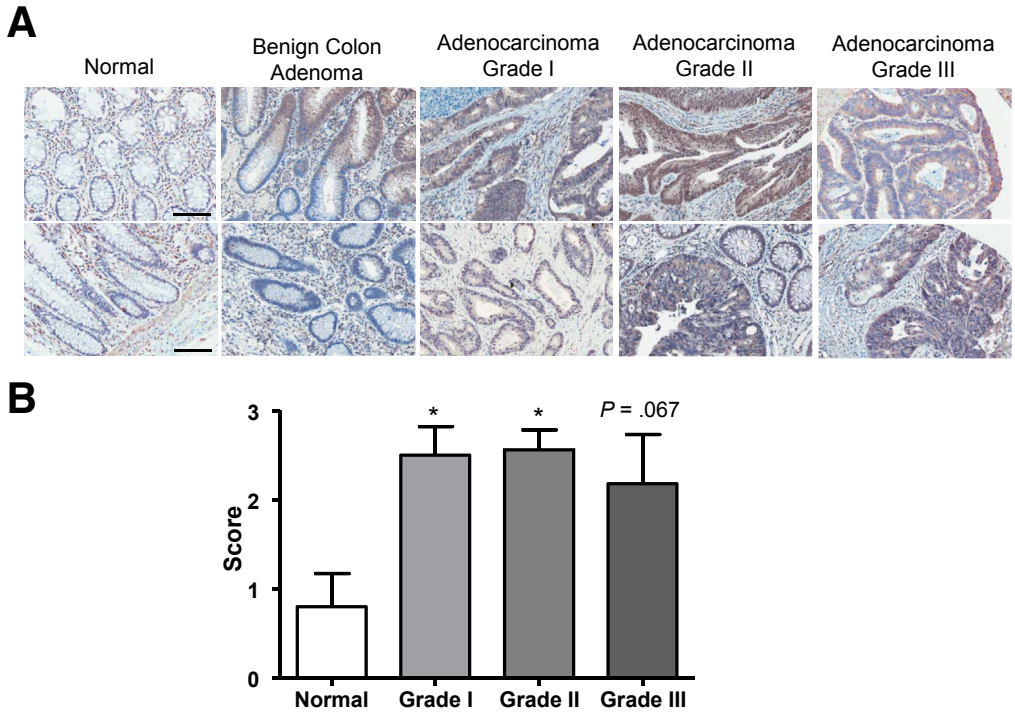

Figure 6. PepT1 expression is up-regulated during colon cancer. (*A*) Human PepT1 antibody was used to observe PepT1 levels in a human tissue microarray counterstained with hematoxylin. The tissue microarray included samples from normal patients, patients with benign colon tumors, and colon cancer patients with various stages of colon adenocarcinoma. (*B*) The anti-human PepT1-stained slides were scored according to 2 parameters (from 0 to 2): the intensity of the staining: 0, absence of PepT1-positive cells; 1, low-intensity staining; and 2, high-intensity staining; and the area of positive cells in the epithelium: 0, absence of PepT1-positive cells; 1, less than the half of the epithelium is PepT1 positive; and 2, half or more of the epithelium is PepT1 positive. The intensity was indexed by the surface parameter giving one final score for each slide. *Scale bars*: 100 μm. *$P < .05$.

colon tumorigenesis, as shown by tumor numbers, sizes, and overall colonic tumor burdens (Figure 7*A–D*), compared with AOM/DSS-only–treated animals. Although both groups of mice lost similar amounts of weight during DSS treatment (Figure 7*E*), KPV-treated mice showed decreased inflammation, fewer aberrant crypt foci, decreased cellular infiltration (as seen on H&E-stained sections), and less epithelial cell proliferation (ie, fewer Ki67$^+$ cells/crypts) (Figure 7*F–H*). To investigate the putative protective effect of KPV administration in PepT1-KO mice, the colitis-associated cancer protocol was modified slightly based on the relative low penetrance of the disease in PepT1-deficient animals (Figure 3). AOM concentration was increased to 15 mg/kg and DSS to 3% to favor tumor development. We observed that, unlike WT mice, PepT1-KO animals were not protected from tumorigenesis by KPV administration, as shown by tumor numbers, sizes, tumor burdens, and mouse body weights that were not changed significantly between AOM/DSS and AOM/DSS + KPV groups (Figure 8*A–E*). Despite the statistical nonsignificance, a trend for a decreased tumor burden index was seen in the KPV-treated group. These data importantly show that KPV acts at least in part through PepT1, opening an important potential therapeutic avenue for the treatment of colonic inflammation and subsequent tumorigenesis.

KPV was shown to decrease tumorigenesis in a colitis-associated model of cancer. We next wanted to know whether KPV also would reduce tumorigenesis in a noninflammatory model. For this purpose, APC$^{Min/+}$ mice, a genetic model of intestinal adenocarcinoma that spontaneously develops adenomas mainly in the small intestine, were treated with KPV for 13 weeks. As presented in Figure 9, KPV did not decrease the tumor burden in the small intestine or in the colon. However, our results importantly showed that intestinal inflammation, assessed by lipocalin-2 measurement, was decreased by KPV treatment, confirming the anti-inflammatory effect of KPV in this model. These results indicated that the decrease of intestinal inflammation induced by KPV, observed in Figure 7, was not sufficient to decrease the tumor formation in a genetic model of tumorigenesis. However, genetic colon carcinoma models only represent 2%–5% of all colon cancers[52] and have a severe tumor development even in germ-free mice and a dramatically decreased basal intestinal inflammation.[53] Therefore, although the inhibition of intestinal inflammation via the KPV/PepT1 pathway was not sufficient to inhibit tumorigenesis in such a stringent model as the APC$^{Min/+}$ mice, KPV showed a promising potential for inhibiting inflammation in various models of colon cancer.

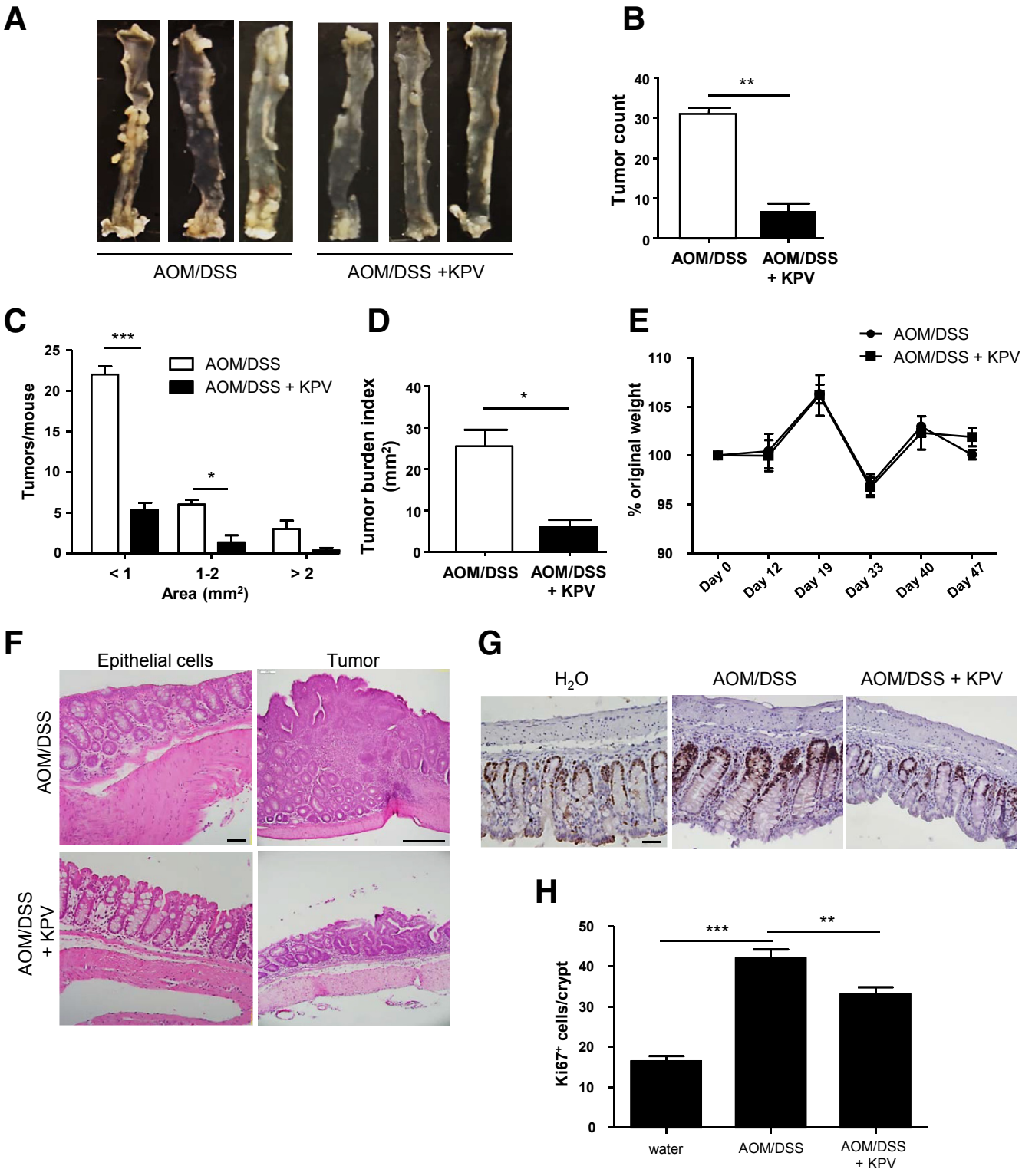

Figure 7. KPV decreases inflammation and tumorigenesis during CAC. WT mice were treated with AOM followed by 2 cycles of DSS, during which mice were co-treated with or without 100 μmol/L KPV. (*A*) Representative colons were obtained from each experimental group at the end of the AOM/DSS protocol. (*B*) Number of tumors per mouse. (*C*) Tumor size was determined using a dissecting microscope fitted with an ocular micrometer. The tumor size distribution was graphed. (*D*) The tumor areas of each colon were summed, and they were presented as the tumor burden index. (*E*) Mice were weighed on day 0, daily during the 2 DSS treatments, and once per week during the 2-week recovery period that followed each DSS or DSS/KPV treatment. The *graph* represents the percentage values of the original day 0 weight. (*F*) Representative images of H&E-stained colonic sections from both experimental groups. (*G*) Epithelial cell proliferation in colonic tissue sections from each experimental group was assessed by immunohistochemistry using the proliferation marker Ki67. (*H*) Ki67$^+$ cells were counted and averaged per crypt. Values are means ± SEM (n = 6 per group). *Scale bars*: 50 μm. *$P < .05$, **$P < .01$, and ***$P < .001$.

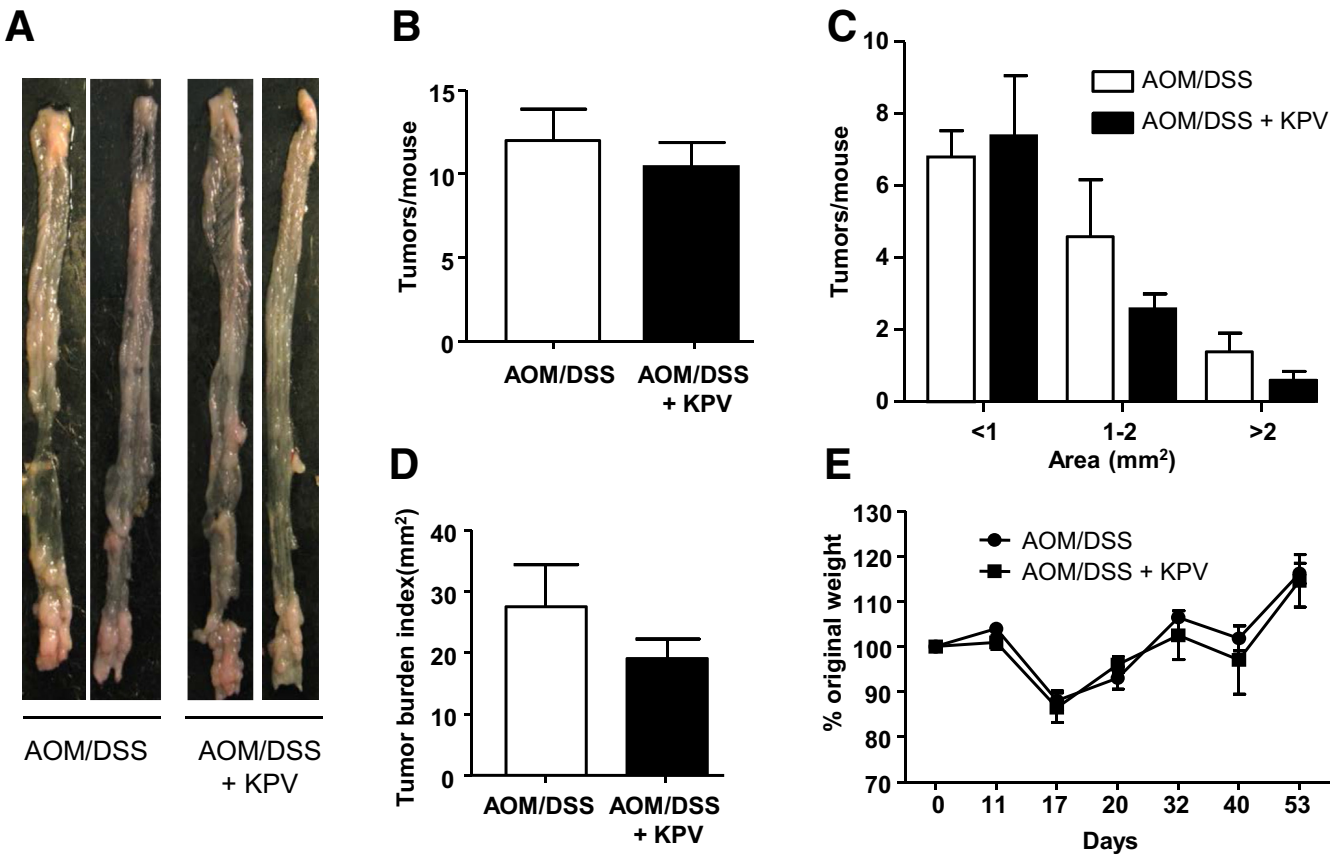

Figure 8. KPV inhibitory effect is abrogated in PepT1-KO mice. PepT1-KO mice were treated with AOM followed by 2 cycles of 3% DSS, during which mice were co-treated with or without 100 μmol/L KPV. (*A*) Representative colons were obtained from each experimental group at the end of the AOM/DSS protocol. (*B*) Number of tumors per mouse. (*C*) Tumor size was determined using a dissecting microscope fitted with an ocular micrometer. The tumor size distribution was graphed. (*D*) The tumor areas of each colon were summed, and they were presented as the tumor burden index. (*E*) Mice were weighed on day 0, daily during the 2 DSS treatments, and once per week during the 2-week recovery period that followed each DSS or DSS/KPV treatment. The *graph* represents the percentage values of the original day 0 weight. Values are means ± SEM (n = 5 per group).

Discussion

The present study showed that PepT1 overexpression leads to increased inflammation and colonic tumor burdens in a murine model of CAC, strongly suggesting that PepT1 plays a crucial role in CAC. Previous reports showed that PepT1 protein expression was up-regulated in the colon under the conditions of chronic inflammation, such as IBD[7,27]; this may increase the interactions between bacterial peptides and intracellular innate immune receptors (eg, NOD receptors), thereby triggering the downstream activation of proinflammatory signaling pathways.[24,54]

In TG mice, we observed up-regulation of proinflammatory cytokines/chemokines and down-regulation of an anti-inflammatory cytokine (IL10) compared with WT mice. It has been reported that IL10-deficient mice develop spontaneous colitis, and after 3 and 6 months, 25% and 60% of the mice develop adenocarcinomas, respectively.[55] Thus, IL10 appears to play an important role in intestinal inflammation. Interestingly, colonic PepT1 protein was expressed in IL10$^{-/-}$ mice that showed signs of colitis, but not in noncolitic IL10$^{-/-}$ mice,[12] suggesting that PepT1 contributes to the development of colitis in this model. In IL10-deficient mice, tumorigenesis was decreased by the administration of exogenous IL10, even after colitis had developed.[31,55] After the induction of the CAC tumor model, we herein found that PepT1-overexpressed TG mice had increased inflammation, larger tumors, and greater overall tumor burdens compared with WT mice, suggesting that PepT1 expression in intestinal epithelial cells may enhance tumor cell growth or survival in the presence of a carcinogenic assault (here, AOM/DSS treatment). Despite the nonsignificance (P = .06), a trend for an increased tumor number was observed in TG mice subjected to AOM/DSS treatment compared with WT. The observation of a subtle increase suggested that the tumor initiation was not the main process being affected by PepT1. Instead, PepT1 appears to enhance the proliferation/survival of tumor cells, contributing to the presence of larger tumors throughout the colon. Consistent with this hypothesis, cell proliferation was increased whereas apoptosis was decreased in the epithelial crypts of TG mice. The tumor number was significantly lower in PepT1-KO mice than in WT mice,

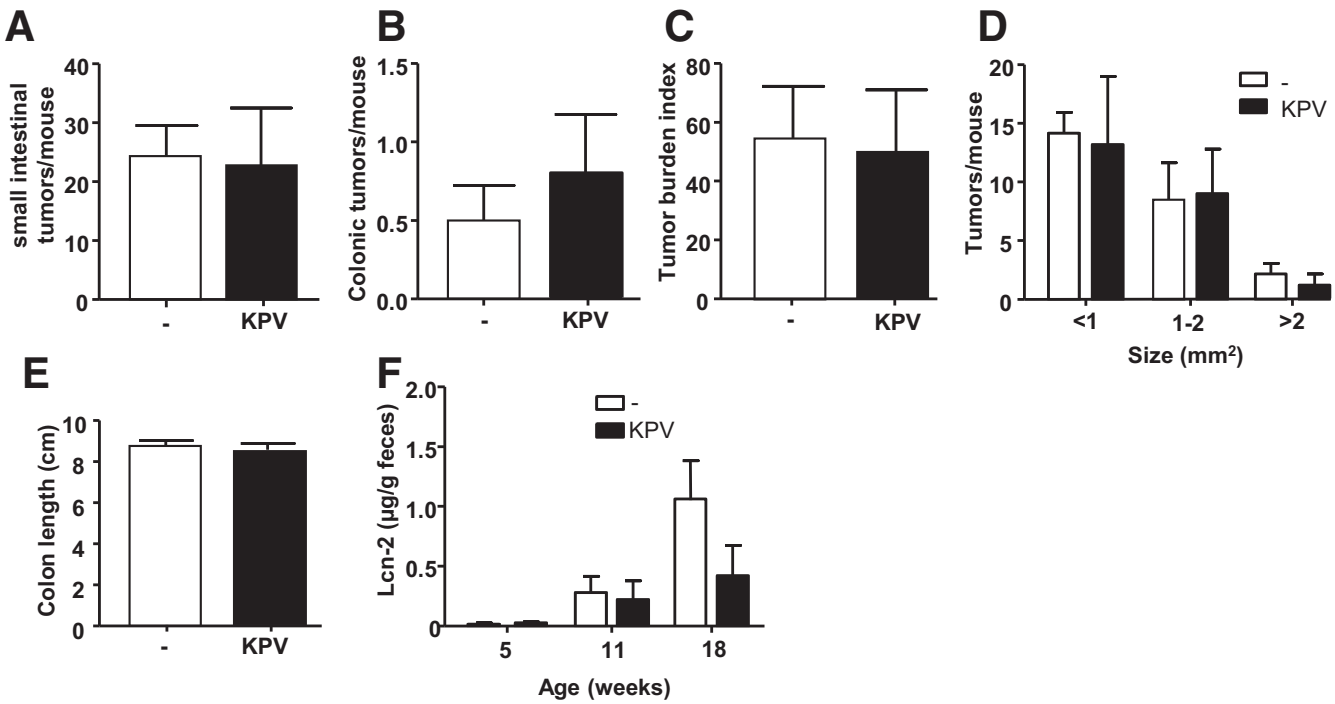

Figure 9. KPV does not reduce tumorigenesis in a genetic model of intestinal cancer. APCMin/+ were treated or not with KPV diluted at a concentration of 100 μmol/L in drinking water. (*A*) Number of small intestinal adenomas per mouse. (*B*) Number of colonic adenomas per mouse. (*C*) Tumor size distribution. (*D*) Spleen weight and (*E*) colon length. (*F*) Lipocalin-2 (LCN-2) was measured in feces collected from 5-week-old, 11-week-old, and 18-week-old mice. Values are means ± SEM (n = 5–6 per group).

however, suggesting that different pathways are involved in the protective effect observed in PepT1-KO mice vs the aggravating effect observed in TG mice. To test this hypothesis, we used Western blot to examine various proteins involved in the prosurvival, proliferation, and tumorigenesis signaling pathways. AOM/DSS treatment enhanced the activation of the NF-κB and Wnt/β-catenin pathways in TG mice compared with WT mice, but no such change was seen in PepT1-KO mice. Conversely, phosphorylated ERK1/2 was similarly up-regulated after AOM/DSS treatment of TG and WT mice, but this up-regulation was abrogated in PepT1-KO mice. This suggests that the absence of PepT1 inhibits the ERK pathway, potentially explaining (at least in part) the inhibition of tumor development and growth observed in PepT1-KO mice.

Because colonic PepT1 is expressed at minimal levels in healthy individuals, treatments that effectively down-regulate PepT1 expression in IBD or, as shown in our study, in CAC patients in whom PepT1 is expressed at higher levels, may attenuate inflammation and reduce the risk for tumorigenesis. For example, treatment of IL10$^{-/-}$ mice with the probiotic *L plantarum* reduced PepT1 expression and activity and attenuated colitis compared with vehicle-treated IL10$^{-/-}$ animals.[12] Alternatively, we showed that PepT1 was up-regulated in colons of mice with AOM/DSS-induced CAC and in human colon adenocarcinoma, and treatments that exploit the transporter activity of PepT1 could increase the effectiveness of particular drugs by enhancing their bioavailability after oral administration. PepT1 transports several types of peptide-derived drugs, including antibiotics, inhibitors of angiotensin-converting enzyme, and anticancer and antiviral drugs.[37,38,56] Among them, the PepT1 substrate and antitumor drug bestatin was found to decrease cell proliferation, ameliorate tumor growth,[57] inhibit the growth of colon adenocarcinoma, and decrease the growth of myeloid leukemia C1498 cells in vivo.[58] In this study, we specifically focused on another peptide, namely KPV.

KPV, a tripeptide from the C-terminus of α-melanocyte–stimulating hormone, confers anti-inflammatory effects,[59,60] acting as a substrate for and actively transported by PepT1 in vitro.[40] After stimulation with proinflammatory cytokines, Caco2-BBE and Jurkat cells that were co-treated with KPV showed attenuated NF-κB activation and decreased proinflammatory cytokine production.[40] Our data presented here, importantly show that KPV treatment is able to decrease AOM/DSS-induced tumorigenesis. This was occurring in a PepT1-dependent manner because PepT1-KO animals were not protected from tumorigenesis by KPV administration. However, a trend for a decreased tumor burden index still was seen in PepT1-KO in the KPV-treated group compared with the water control group, pointing out that, even if mainly PepT1-dependent, KPV also might be transported by other peptide transporters. KPV still represents a promising drug for targeting PepT1, as inferred from a previous study that found a high affinity of hPepT1 for KPV (Km ~ 160 μmol/L) in Caco2-BBE cells.[40] This Km is among the lowest Kms reported for hPepT1. For example,

Gly-Sar, which is the most commonly used PepT1 substrate, has a Km of 1 mmol/L or greater in Caco2-BBE cells.[61] This will allow low doses of KPV to be transported efficiently by PepT1. This aspect is of high interest for using this tripeptide in clinics for the treatment of IBD or CAC.

IBD-related inflammation is believed to increase the risk of colorectal cancer, but many existing studies have failed to show a strong positive link between the anti-inflammatory drugs commonly used to treat IBD and a decreased risk of colon cancer.[62] However, a long-term reduction of the inflammation by the use of nonsteroidal anti-inflammatory drugs was associated previously with a protective role against colorectal cancer.[63] In the present study, we reported a time-dependent increase of intestinal inflammation in $APC^{Min/+}$. Importantly, even with a limited inhibition of tumorigenesis in such a stringent model, KPV was sufficient to decrease the inflammation in this model of non–inflammatory-induced carcinogenesis. Therefore, we anticipate that the use of KPV before the development of colon cancer might be of interest as a preventive agent of colonic carcinogenesis.

Overall, additional studies are warranted to determine the precise mechanism by which KPV decreases tumorigenesis in this model, and to test whether this tripeptide could be beneficial against human CAC.

Finally, several studies have shown that PepT1 is expressed by cancer cell types beyond colorectal cancer cells,[64–66] including gastric and pancreatic cancer cells. Thus, the transporter activity of PepT1 in either the small or large intestine may be used to address these other types of cancer, and future studies may identify other tumor types that show increased PepT1 expression.

References

1. Daniel H, Kottra G. The proton oligopeptide cotransporter family SLC15 in physiology and pharmacology. Pflugers Arch 2004;447:610–618.
2. Ingersoll SA, Ayyadurai S, Charania MA, et al. The role and pathophysiological relevance of membrane transporter PepT1 in intestinal inflammation and inflammatory bowel disease. Am J Physiol Gastrointest Liver Physiol 2012;302:G484–G492.
3. Drozdzik M, Groer C, Penski J, et al. Protein abundance of clinically relevant multidrug transporters along the entire length of the human intestine. Mol Pharm 2014; 11:3547–3555.
4. Englund G, Rorsman F, Ronnblom A, et al. Regional levels of drug transporters along the human intestinal tract: co-expression of ABC and SLC transporters and comparison with Caco-2 cells. Eur J Pharm Sci 2006; 29:269–277.
5. Jappar D, Wu SP, Hu Y, et al. Significance and regional dependency of peptide transporter (PEPT) 1 in the intestinal permeability of glycylsarcosine: in situ single-pass perfusion studies in wild-type and Pept1 knockout mice. Drug Metab Dispos 2010; 38:1740–1746.
6. Meier Y, Eloranta JJ, Darimont J, et al. Regional distribution of solute carrier mRNA expression along the human intestinal tract. Drug Metab Dispos 2007; 35:590–594.
7. Merlin D, Si-Tahar M, Sitaraman SV, et al. Colonic epithelial hPepT1 expression occurs in inflammatory bowel disease: transport of bacterial peptides influences expression of MHC class 1 molecules. Gastroenterology 2001;120:1666–1679.
8. Ogihara H, Saito H, Shin BC, et al. Immuno-localization of H+/peptide cotransporter in rat digestive tract. Biochem Biophys Res Commun 1996;220:848–852.
9. Ziegler TR, Fernandez-Estivariz C, Gu LH, et al. Distribution of the H+/peptide transporter PepT1 in human intestine: up-regulated expression in the colonic mucosa of patients with short-bowel syndrome. Am J Clin Nutr 2002;75:922–930.
10. Ma K, Hu Y, Smith DE. Influence of fed-fasted state on intestinal PEPT1 expression and in vivo pharmacokinetics of glycylsarcosine in wild-type and Pept1 knockout mice. Pharm Res 2012;29:535–545.
11. Wuensch T, Schulz S, Ullrich S, et al. The peptide transporter PEPT1 is expressed in distal colon in rodents and humans and contributes to water absorption. Am J Physiol Gastrointest Liver Physiol 2013;305:G66–G73.
12. Chen HQ, Yang J, Zhang M, et al. Lactobacillus plantarum ameliorates colonic epithelial barrier dysfunction by modulating the apical junctional complex and PepT1 in IL-10 knockout mice. Am J Physiol Gastrointest Liver Physiol 2010;299:G1287–G1297.
13. Nguyen HT, Dalmasso G, Powell KR, et al. Pathogenic bacteria induce colonic PepT1 expression: an implication in host defense response. Gastroenterology 2009; 137:1435–1447, e1-2.
14. Merlin D, Steel A, Gewirtz AT, et al. hPepT1-mediated epithelial transport of bacteria-derived chemotactic peptides enhances neutrophil-epithelial interactions. J Clin Invest 1998;102:2011–2018.
15. Charrier L, Driss A, Yan Y, et al. hPepT1 mediates bacterial tripeptide fMLP uptake in human monocytes. Lab Invest 2006;86:490–503.
16. Buyse M, Tsocas A, Walker F, et al. PepT1-mediated fMLP transport induces intestinal inflammation in vivo. Am J Physiol Cell Physiol 2002;283:C1795–C1800.
17. Shi B, Song D, Xue H, et al. Abnormal expression of the peptide transporter PepT1 in the colon of massive bowel resection rat: a potential route for colonic mucosa damage by transport of fMLP. Dig Dis Sci 2006; 51:2087–2093.
18. Wang P, Lu YQ, Wen Y, et al. IL-16 induces intestinal inflammation via PepT1 upregulation in a pufferfish model: new insights into the molecular mechanism of inflammatory bowel disease. J Immunol 2013; 191:1413–1427.
19. Wu SP, Smith DE. Impact of intestinal PepT1 on the kinetics and dynamics of N-formyl-methionyl-leucyl-phenylalanine, a bacterially-produced chemotactic peptide. Mol Pharm 2013;10:677–684.
20. Vavricka SR, Musch MW, Chang JE, et al. hPepT1 transports muramyl dipeptide, activating NF-kappaB and stimulating IL-8 secretion in human colonic Caco2/bbe cells. Gastroenterology 2004;127:1401–1409.

21. Dalmasso G, Nguyen HT, Charrier-Hisamuddin L, et al. PepT1 mediates transport of the proinflammatory bacterial tripeptide L-Ala-{gamma}-D-Glu-meso-DAP in intestinal epithelial cells. Am J Physiol Gastrointest Liver Physiol 2010;299:G687–G696.
22. Ayyadurai S, Charania MA, Xiao B, et al. Colonic miRNA expression/secretion, regulated by intestinal epithelial PepT1, plays an important role in cell-to-cell communication during colitis. PLoS One 2014;9:e87614.
23. Zucchelli M, Torkvist L, Bresso F, et al. PepT1 oligopeptide transporter (SLC15A1) gene polymorphism in inflammatory bowel disease. Inflamm Bowel Dis 2009; 15:1562–1569.
24. Dalmasso G, Nguyen HT, Ingersoll SA, et al. The PepT1-NOD2 signaling pathway aggravates induced colitis in mice. Gastroenterology 2011;141:1334–1345.
25. Ayyadurai S, Charania MA, Xiao B, et al. PepT1 expressed in immune cells has an important role in promoting the immune response during experimentally induced colitis. Lab Invest 2013;93:888–899.
26. Weir HK, Thun MJ, Hankey BF, et al. Annual report to the nation on the status of cancer, 1975-2000, featuring the uses of surveillance data for cancer prevention and control. J Natl Cancer Inst 2003;95:1276–1299.
27. Wojtal KA, Eloranta JJ, Hruz P, et al. Changes in mRNA expression levels of solute carrier transporters in inflammatory bowel disease patients. Drug Metab Dispos 2009;37:1871–1877.
28. Eaden JA, Abrams KR, Mayberry JF. The risk of colorectal cancer in ulcerative colitis: a meta-analysis. Gut 2001;48:526–535.
29. Ahmadi A, Polyak S, Draganov PV. Colorectal cancer surveillance in inflammatory bowel disease: the search continues. World J Gastroenterol 2009;15:61–66.
30. Feagins LA, Souza RF, Spechler SJ. Carcinogenesis in IBD: potential targets for the prevention of colorectal cancer. Nat Rev Gastroenterol Hepatol 2009;6:297–305.
31. Ullman TA, Itzkowitz SH. Intestinal inflammation and cancer. Gastroenterology 2011;140:1807–1816.
32. Ekbom A, Helmick C, Zack M, et al. Increased risk of large-bowel cancer in Crohn's disease with colonic involvement. Lancet 1990;336:357–359.
33. Jess T, Gamborg M, Matzen P, et al. Increased risk of intestinal cancer in Crohn's disease: a meta-analysis of population-based cohort studies. Am J Gastroenterol 2005;100:2724–2729.
34. Thorsteinsdottir S, Gudjonsson T, Nielsen OH, et al. Pathogenesis and biomarkers of carcinogenesis in ulcerative colitis. Nat Rev Gastroenterol Hepatol 2011; 8:395–404.
35. Chen J, Huang XF. The signal pathways in azoxymethane-induced colon cancer and preventive implications. Cancer Biol Ther 2009;8:1313–1317.
36. De Robertis M, Massi E, Poeta ML, et al. The AOM/DSS murine model for the study of colon carcinogenesis: from pathways to diagnosis and therapy studies. J Carcinog 2011;10:9.
37. Adibi SA. Regulation of expression of the intestinal oligopeptide transporter (Pept-1) in health and disease. Am J Physiol Gastrointest Liver Physiol 2003; 285:G779–G788.
38. Thwaites DT, Anderson CM. H+-coupled nutrient, micronutrient and drug transporters in the mammalian small intestine. Exp Physiol 2007;92:603–619.
39. Newstead S. Towards a structural understanding of drug and peptide transport within the proton-dependent oligopeptide transporter (POT) family. Biochem Soc Trans 2011;39:1353–1358.
40. Dalmasso G, Charrier-Hisamuddin L, Nguyen HT, et al. PepT1-mediated tripeptide KPV uptake reduces intestinal inflammation. Gastroenterology 2008;134:166–178.
41. Luger TA, Scholzen TE, Brzoska T, et al. New insights into the functions of alpha-MSH and related peptides in the immune system. Ann N Y Acad Sci 2003; 994:133–140.
42. Brzoska T, Luger TA, Maaser C, et al. Alpha-melanocyte-stimulating hormone and related tripeptides: biochemistry, antiinflammatory and protective effects in vitro and in vivo, and future perspectives for the treatment of immune-mediated inflammatory diseases. Endocr Rev 2008;29:581–602.
43. Laroui H, Dalmasso G, Nguyen HT, et al. Drug-loaded nanoparticles targeted to the colon with polysaccharide hydrogel reduce colitis in a mouse model. Gastroenterology 2010;138:843–853, e1-2.
44. Kannengiesser K, Maaser C, Heidemann J, et al. Melanocortin-derived tripeptide KPV has anti-inflammatory potential in murine models of inflammatory bowel disease. Inflamm Bowel Dis 2008;14:324–331.
45. Greten FR, Eckmann L, Greten TF, et al. IKKbeta links inflammation and tumorigenesis in a mouse model of colitis-associated cancer. Cell 2004;118:285–296.
46. Viennois E, Xiao B, Ayyadurai S, et al. Micheliolide, a new sesquiterpene lactone that inhibits intestinal inflammation and colitis-associated cancer. Lab Invest 2014; 94:950–965.
47. Wong NA, Pignatelli M. Beta-catenin–a linchpin in colorectal carcinogenesis? Am J Pathol 2002;160:389–401.
48. DiDonato JA, Mercurio F, Karin M. NF-kappaB and the link between inflammation and cancer. Immunol Rev 2012;246:379–400.
49. Lengyel E, Wang H, Gum R, et al. Elevated urokinase-type plasminogen activator receptor expression in a colon cancer cell line is due to a constitutively activated extracellular signal-regulated kinase-1-dependent signaling cascade. Oncogene 1997;14:2563–2573.
50. Rice PL, Goldberg RJ, Ray EC, et al. Inhibition of extracellular signal-regulated kinase 1/2 phosphorylation and induction of apoptosis by sulindac metabolites. Cancer Res 2001;61:1541–1547.
51. Hagiya Y, Fukuhara H, Matsumoto K, et al. Expression levels of PEPT1 and ABCG2 play key roles in 5-aminolevulinic acid (ALA)-induced tumor-specific protoporphyrin IX (PpIX) accumulation in bladder cancer. Photodiagnosis Photodyn Ther 2013;10:288–295.
52. Jasperson KW, Tuohy TM, Neklason DW, et al. Hereditary and familial colon cancer. Gastroenterology 2010; 138:2044–2058.

53. Li Y, Kundu P, Seow SW, de Matos CT, et al. Gut microbiota accelerate tumor growth via c-jun and STAT3 phosphorylation in APCMin/+ mice. Carcinogenesis 2012;33:1231–1238.
54. Laroui H, Yan Y, Narui Y, et al. L-Ala-gamma-D-Glu-meso-diaminopimelic acid (DAP) interacts directly with leucine-rich region domain of nucleotide-binding oligomerization domain 1, increasing phosphorylation activity of receptor-interacting serine/threonine-protein kinase 2 and its interaction with nucleotide-binding oligomerization domain 1. J Biol Chem 2011;286:31003–31013.
55. Berg DJ, Davidson N, Kuhn R, et al. Enterocolitis and colon cancer in interleukin-10-deficient mice are associated with aberrant cytokine production and CD4(+) TH1-like responses. J Clin Invest 1996;98:1010–1020.
56. Adibi SA. The oligopeptide transporter (Pept-1) in human intestine: biology and function. Gastroenterology 1997;113:332–340.
57. Nielsen CU, Brodin B. Di/tri-peptide transporters as drug delivery targets: regulation of transport under physiological and patho-physiological conditions. Curr Drug Targets 2003;4:373–388.
58. Abe F, Shibuya K, Uchida M, et al. Effect of bestatin on syngeneic tumors in mice. Gan 1984;75:89–94.
59. Hiltz ME, Lipton JM. Antiinflammatory activity of a COOH-terminal fragment of the neuropeptide alpha-MSH. FASEB J 1989;3:2282–2284.
60. Kelly JM, Moir AJ, Carlson K, et al. Immobilized alpha-melanocyte stimulating hormone 10-13 (GKPV) inhibits tumor necrosis factor-alpha stimulated NF-kappaB activity. Peptides 2006;27:431–437.
61. Brandsch M, Miyamoto Y, Ganapathy V, et al. Expression and protein kinase C-dependent regulation of peptide/H+ co-transport system in the Caco-2 human colon carcinoma cell line. Biochem J 1994;299:253–260.
62. Farraye FA, Odze RD, Eaden J, et al. AGA technical review on the diagnosis and management of colorectal neoplasia in inflammatory bowel disease. Gastroenterology 2010;138:746–774, 774 e1–4; quiz e12–e13.
63. Bansal P, Sonnenberg A. Risk factors of colorectal cancer in inflammatory bowel disease. Am J Gastroenterol 1996;91:44–48.
64. Inoue M, Terada T, Okuda M, et al. Regulation of human peptide transporter 1 (PEPT1) in gastric cancer cells by anticancer drugs. Cancer Lett 2005;230:72–80.
65. Mitsuoka K, Kato Y, Miyoshi S, et al. Inhibition of oligopeptide transporter suppress growth of human pancreatic cancer cells. Eur J Pharm Sci 2010;40:202–208.
66. Gonzalez DE, Covitz KM, Sadee W, et al. An oligopeptide transporter is expressed at high levels in the pancreatic carcinoma cell lines AsPc-1 and Capan-2. Cancer Res 1998;58:519–525.

Received June 25, 2015. Accepted January 9, 2016.

Correspondence
Address correspondence to: Emilie Viennois, PhD, Institute for Biomedical Sciences, Georgia State University, 100 Piedmont Avenue, PSC 757, Atlanta, Georgia 30303. e-mail: eviennois@gsu.edu; fax: (404) 413-3580.

Conflicts of interest
The authors disclose no conflicts.

Funding
Supported by grants from the Department of Veterans Affairs (BX002526) and the National Institute of Diabetes and Digestive and Kidney Diseases (RO1-DK-071594 to D.M.); Research Fellowship Award from the Crohn's & Colitis Foundation of America (to E.V. and M.Z.); and a Research Career Scientist Award from the Department of Veterans Affairs (D.M.).